Journal of Catalysis **185,** 160–169 (1999)
Article ID jcat.1999.2491, available online at http://www.idealibrary.com on IDEAL®

Generation and Reactions of CH_2 and C_2H_5 Species on Mo_2C/Mo(111) Surface

F. Solymosi, L. Bugyi, A. Oszkó, and I. Horváth

Institute of Solid State and Radiochemistry, Attila József University, and Reaction Kinetics Research Group, Hungarian Academy of Sciences, Center for Catalysis, Surface, and Material Science, University of Szeged, P.O. Box 168, H-6701 Szeged, Hungary

Received December 7, 1998; revised March 9, 1999; accepted March 11, 1999

The adsorption and dissociation of CH_2I_2 and C_2H_5I on Mo_2C/Mo(111) surface have been investigated with the purpose of producing adsorbed CH_2 and C_2H_5 species. Methods used include high resolution electron energy loss, X-ray photoelectron, Auger electron, and temperature programmed desorption spectroscopies. Independently of the coverage, CH_2I_2 adsorbs molecularly at 90–100 K. The dissociation of an adsorbed layer starts around 180–190 K. The primary products of thermal dissociation are adsorbed CH_2 and I. The species CH_2 undergoes self-hydrogenation to CH_4 at $T_p = 300$ K and dimerization into C_2H_4 at and above 222–280 K. Ethylene formed desorbs above 400 K. C_2H_5I also adsorbs molecularly on Mo_2C at 90–100 K and dissociates to C_2H_5 and I above 150 K. The reaction of C_2H_5 on Mo_2C/Mo(111) surface yielding C_2H_6 and C_2H_4 proceeds at a much lower temperature, above 180 K, than that of CH_2. Neither the cleavage of the C–C bond nor the coupling of C_2 compounds occurred to detectable extent under the reaction conditions. The ethylene formed in the reactions of both CH_x species exhibited the same features as observed following C_2H_4 adsorption on Mo_2C: the stable di-σ-bonded ethylene is transformed into ethylidyne at higher temperature. The results are discussed in relevance to the conversion of methane into benzene on Mo_2C deposited on ZSM-5.

1. INTRODUCTION

It has been recognized for a long time that the synthesis of hydrocarbons proceeds by the coupling and polymerization of the smallest hydrocarbon fragments on the catalyst surface. These hydrocarbon species (CH_2, CH_3, C_2H_5, etc.) play a dominant role in the partial and complete oxidation of hydrocarbons, in the synthesis of methanol and oxygenated hydrocarbons and also in the oxidative coupling of methane (1, 2). The more detailed study of the surface chemistry of C_xH_y species was hindered by the difficulty of preparing them in given and large concentrations on the catalyst surfaces. This difficulty was recently overcome by the application of halogenated hydrocarbons, the dissociation of which generated the desired C_xH_y compounds in relatively high surface concentration (3–13).

Studies performed so far show that Pt metals are very active in the decomposition of C_xH_y compounds into surface carbon. The reaction pathways can be altered, however, by different promotors, such as potassium and zinc (14–16). On Cu and Ag surfaces, the coupling of C_xH_y is the dominant reaction route (8). In consistence with this behavior, supported Pt metals are effective in the complete decomposition of methane—with only a very limited formation of C_2H_6 and C_2H_4—while the decomposition of CH_4 cannot be initiated in the same temperature range by supported Cu and Ag catalysts (17–25).

In the present work an account is given on the chemistry of CH_2 and C_2H_5 on Mo_2C/Mo(111) surface, which is a continuation of our previous work dealing with the chemistry of CH_3 on the same surface (26). The motivation of this study is that Mo_2C deposited on ZSM-5 is an effective catalyst in the conversion of methane into benzene (27–30). High activity was also exhibited for this reaction by MoO_3 and MoO_2 on ZSM-5, but both Mo oxides have been converted into Mo_2C during the high temperature reaction, which is the actual catalyst for this process (27–33). As regards the role of Mo_2C it was assumed that it activates the CH_4 molecule to give CH_3 or CH_2 species, which may dimerize on the Mo_2C or migrate onto the ZSM-5, where ethane or ethylene are produced. The aromatization of these compounds proceeds on the acidic sites of ZSM-5.

2. EXPERIMENTAL

The experiments were performed in two separate UHV chambers with a routine base pressure of 2×10^{-9} mbar produced by turbomolecular, ion-getter, and titanium sublimation pumps. One chamber was equipped with facilities for Auger electron spectroscopy (AES), high resolution electron energy loss spectroscopy (HREELS), and temperature programmed desorption (TPD). The HREEL spectrometer (VSW, type HA-50) is situated in the lower level of the chamber and has a resolution of 70–100 cm^{-1}. All spectra reported were recorded with a primary energy of 5.0 eV and at an incident angle of 45°. Work function changes,

0021-9517/99 $30.00

based on secondary electron energy threshold, were measured with the same electron gun and analyzer used in HREELS. The second system was a Kratos XSAM 800 instrument, where X-ray photoelectron spectroscopy (XPS) measurements were performed using Al$K\alpha$ primary radiation (14 kV, 10 mA). All binding energies are referred to the Fermi level which places the Mo($3d_{5/2}$) photoelectron line at 227.2 eV. The pass energy of the electron energy analyzer was set to 40 eV which gives the full width at half maximum (FWHM) of 1.15 eV for the Mo($3d_{5/2}$) photoelectron line for a clean Mo(111) surface. Collection times for XPS were 15 and 30 min, respectively.

The Mo(111) crystal used in this work was a product of Materials Research Corporation (purity 99.99%). Initially the sample was cleaned by cycled heating in oxygen. This was followed by cycles of argon-ion bombardment (typically 1–2 kV, 1×10^{-7} Torr Ar, 1000 K, 10 μA for 10–30 min) and annealing at 1270 K for several minutes. Mo_2C/Mo(111) surface was prepared by the method of Schöberl (34). The Mo(111) surface was exposed to 200 L of ethylene at 900 K. The resulting surface as checked by XPS and AES turned out to be carbidic, showing the characteristic three-lobe line shape of carbidic carbon in AES at 255.6, 262.1, and 272.7 eV and the C(1s) peak at 282.7 eV in the XPS (34). The ratio of $C_{272.7}/Mo_{186}$ signals in AES for carbidized Mo(111) was 0.5. These values—using exactly the same procedure for preparation—were very well reproducible. The Mo_2C layer so prepared is disorganized (34). CH_2I_2 and C_2H_5I were the products of Merck, which were degassed and purified by freeze–pump–thaw cycles.

3. RESULTS

3.1. CH_2I_2

3.1.1. Work function measurements. The adsorption of CH_2I_2 on Mo_2C/Mo(111) caused a linear decrease in the work function of the sample (Fig. 1A) up to about 1.5 L of exposure. The maximum work function decrease was 0.9 eV. Further exposure led to an increase of work function by about 0.3 eV. Annealing of the sample containing a multilayer of CH_2I_2 first caused a sudden increase in the work function value at 150–200 K (Fig. 1B). Afterward the work function remained constant up to 400 K. A more significant increase was observed above 500 K. The initial value of the Mo_2C/Mo(111) surface was attained around 1000 K. The I AES signal disappeared at nearly the same temperature.

3.1.2. XPS measurements. Independently of the exposure the binding energy of I($3d_{5/2}$) was registered at 620.1 eV. The area of the I peak at 620.1 eV increased linearly with the rise of CH_2I_2 exposure. In the C(1*s*) region, the adsorption of CH_2I_2 yielded a new broad peak centered at 285.1 eV, the position of which also remained unaltered with the increase of the exposure.

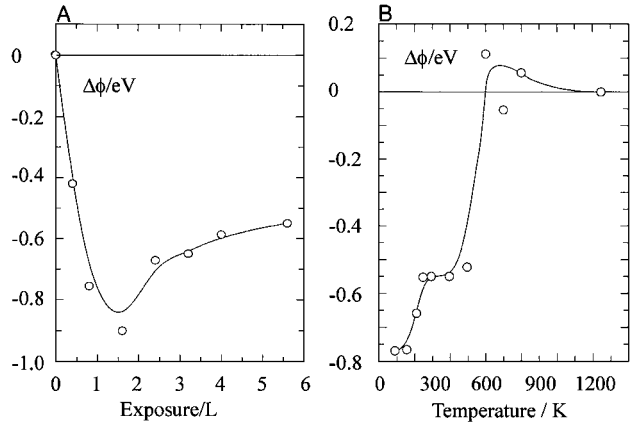

FIG. 1. Changes in the work function ($\Delta\phi$) of Mo_2C/Mo(111) as a function of CH_2I_2 exposure at 100 K (A) and annealing temperature (B).

Selected XPS spectra of adsorbed layers annealed at different temperatures are displayed in Fig. 2A. Annealing of a multilayer up to 170 K caused a slight change in the position of I($3d_{5/2}$) at 620.1 eV. At 190 K, a significant attenuation of both the I($3d_{5/2}$) and the C(1*s*) signals was observed. A new peak at 618.7 eV was seen first at 190 K which became more intense at higher temperature with the simultaneous reduction of the high energy peak at 620.1 eV. This latter peak was eliminated above 250 K.

Fewer changes were experienced in the position of the C(1*s*) signal caused by the adsorption of CH_2I_2. At 150 K it centered at 285.0 eV, and above 200 K at 283.9 eV. The intensity of the peak radically decreased when the adsorbed layer was heated above 200 K.

3.1.3. TPD measurements. Figure 3A shows TPD spectra of CH_2I_2 at different dosing times on Mo_2C/Mo(111). Desorption of molecularly adsorbed CH_2I_2 was observed above 1.0 L of exposure; a single desorption peak developed with $T_p = 195$ K. The position of the peak remained practically unaltered with increasing CH_2I_2 exposure and did not saturate even at high CH_2I_2 doses. The activation energy of the desorption calculated by the Redhead formula is 50 kJ/mol.

Besides the desorption of CH_2I_2, the formation of CH_4, C_2H_4, and H_2 was also established. The methane peak was registered at 300–320 K (Fig. 3D). At low coverage, ethylene desorbed with $T_p = 530$ K. At higher coverages a low temperature peak also developed at $T_p = 440$ K (Fig. 3C). The desorption of H_2 occurred in two stages with $T_p = 380$–400 K and 570–580 K. Attempts to detect the formation of other hydrocarbon products (acetylene and ethane) did not bring positive results. The desorption of iodine was also followed: it was released above 1000 K with a $T_p = 1100$ K. The amount of desorbed iodine is proportional to the amount of CH_2I_2 decomposed. Characteristic data for thermal desorption of CH_2I_2 and its decomposition products are collected in Table 1.

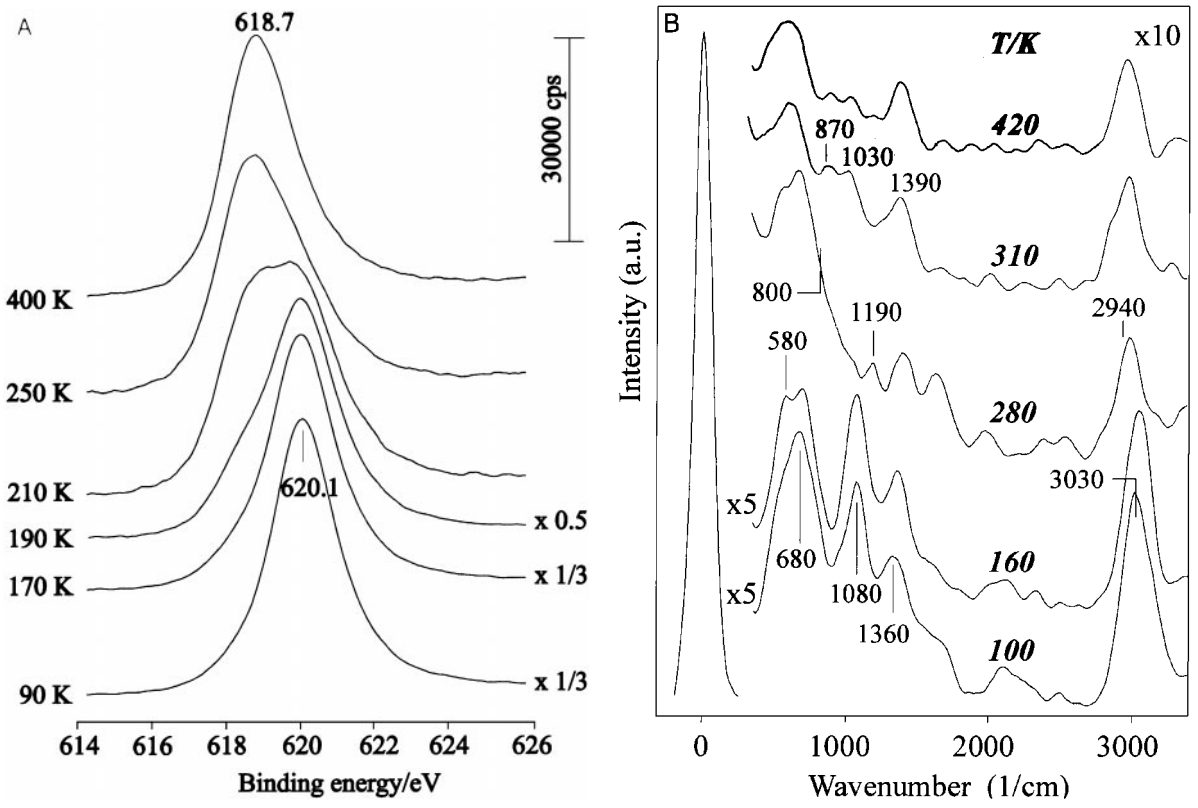

FIG. 2. Effects of annealing on (A) the XPS spectra of I($3d_{5/2}$) and (B) on HREEL spectra of adsorbed CH_2I_2.

Some measurements have been performed as concerns the effect of adsorption temperature on the product distribution. In order to obtain a more reliable picture, the amount of ethylene and methane formed was related to that of the iodine desorbed above 1000 K, in other words, to the extent of CH_2I_2 decomposition. The values obtained are listed in Table 2. It shows clearly that the relative amount of ethylene is enhanced by a factor of 5 when the adsorption temperature of CH_2I_2 has been increased from 100 to 300 K.

TABLE 1

Characteristic Thermal Desorption Data for CH_2I_2 and C_2H_5I on Mo_2C/Mo(111)

	T_p (K)	E (kJ/mol)
CH_2I_2/desorbing species		
CH_2I_2	195	50
H_2		
α	400	100
β	580	146
C_2H_4		
α	440	110
β	540	136
CH_4	300	75
C_2H_5I/desorbing species		
C_2H_5I	145	36
H_2		
α	405	100
β	580	146
C_2H_4		
α	230–270	62
β	455–545	110–136
C_2H_6	250	62

3.1.4. HREELS measurements. HREEL spectra were recorded in the specular direction for CH_2I_2 as a function of exposure at 100 K. Before exposure to CH_2I_2, the Mo_2C/Mo(111) surface exhibited a single Mo–C stretching

TABLE 2

Effects of Adsorption Temperature on the Relative Amounts of Products Formed in the Reaction of CH_2 and C_2H_5

	$T_a = 100$ K	$T_a = 300$ K
Mo_2C/Mo(111) + CH_2I_2		
C_2H_4/I_2	1.8	8.6
CH_4/I_2	35	7.4
C_2H_4/H_2[a]	0.02	0.3
Mo_2C/Mo(111) + C_2H_5I		
β-C_2H_4/I_2	12.7	20
C_2H_6/I_2	7.0	0.0
β-C_2H_4/H_2[a]	0.03	0.015

[a] These values are less reliable due to the presence of hydrogen in the background.

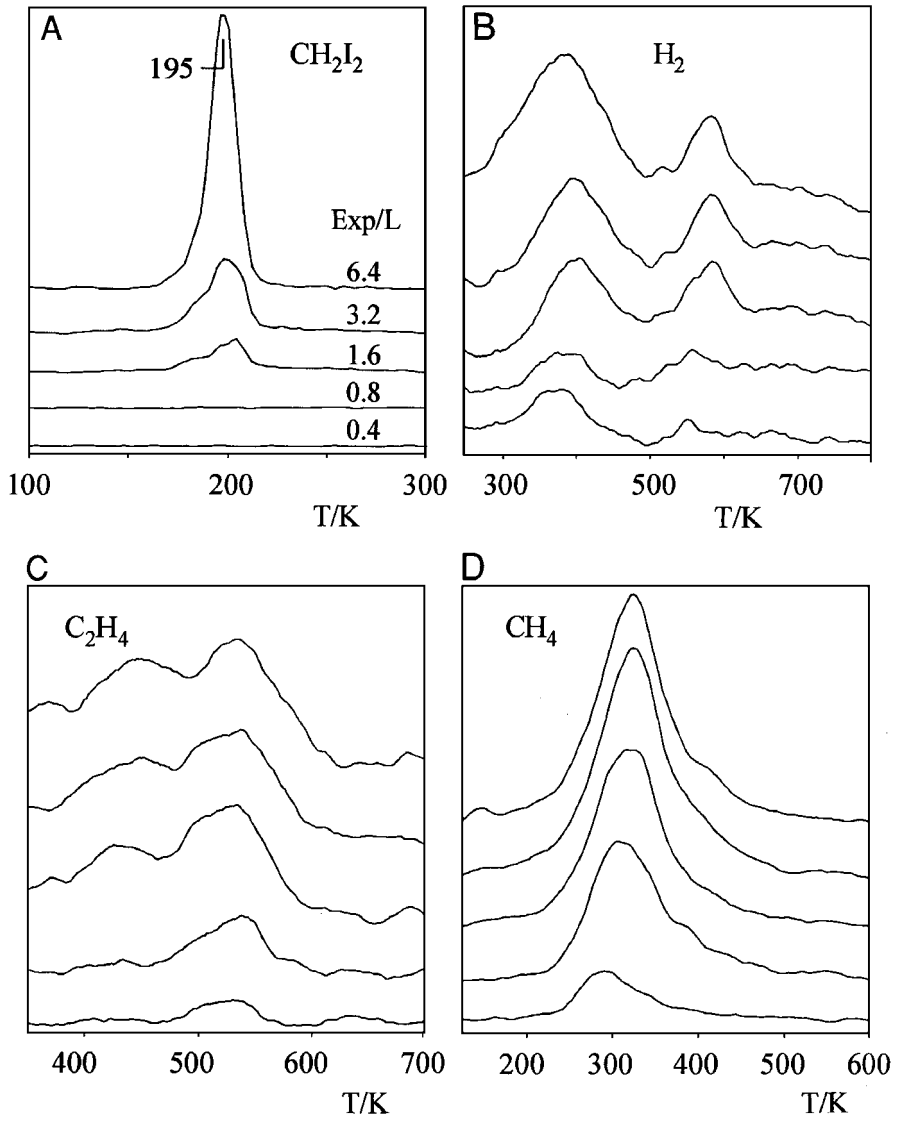

FIG. 3. TPD spectra following CH_2I_2 adsorption on Mo_2C/Mo(111) at 100 K as a function of CH_2I_2 exposure. (A) CH_2I_2; (B) H_2; (C) C_2H_4; (D) CH_4.

vibration at ~400 cm^{-1}. New vibration losses were registered at 3030, 1360, 1080, ~675, and ~580 cm^{-1} (Fig. 2B). All the losses gained intensity with the increase of the exposure, but the positions of the losses remained practically constant. Characteristic loss features for CH_2I_2 adsorbed on the Mo_2C/Mo(111) surface are listed in Table 3.

The HREELS annealing set of adsorbed CH_2I_2 on Mo_2C sample is shown in Fig. 2B. A significant attenuation of the peaks was experienced above 160 K. Further heating to 280 K caused a clear appearance of a new loss feature at 1190 cm^{-1} and the broadening of the peak around 700 cm^{-1} toward higher energy and the shift of the peak at 3030 cm^{-1} toward lower energy. Note that after a long data collection time a broad feature developed at 1640 cm^{-1} which we attribute to the vibration of H_2O adsorbed from the background.

In order to increase the surface concentration of adsorbed species present at and above 300 K, in the subsequent measurements the adsorption of CH_2I_2 was performed at 310 K. Spectra obtained are also shown in Fig. 2B. Vibrational features were found at 1390, 1030, 870–900, and 630 cm^{-1}. After heating the surface to 420 K, only slight changes were experienced in the positions of these peaks. Above 420 K, a significant attenuation of the losses occurred, which made their resolution difficult, but weak features at 2925, 1430, 920, and 525 cm^{-1} could be seen.

3.2. C_2H_5I

3.2.1. Work function measurements. The adsorption of C_2H_5I on Mo_2C/Mo(111) caused a sharp decrease in the work function of Mo_2C up to about 1.0 L of C_2H_5I exposure

TABLE 3

Vibrational Characteristics for Gaseous CH_2I_2 and Adsorbed CH_2I_2 and CH_2

Assignment	$CH_2I_{2(g)}$ (43)	CH_2I_2/Rh(111) at 100 K (43)	CH_2/Rh(111) (8, 43)	CH_2I_2/Mo_2C/Mo(111) at 100 K (present work)	di-σ-C_2H_4/(4 × 4)-C/Mo(110) (44)
$\nu_{as}(CH_2)$	3047	3030	2940	3030	3010
$\nu_s(CH_2)$	2968	2940	—		2935
$\delta(CH_2)$	1353	1350	—	1360	1395
$\omega(CH_2)$	—	—	1190	—	1180
$\gamma(CH_2)$	1106	1080	—	1080	1035
$\rho(CH_2)$	717	720	780	675	905
$\nu_{as}(C\text{-}I_2)$	571	560	—	580	—
$\nu_s(C\text{-}I_2)$	486	—	—	—	—
$\nu_s(M\text{-}C)$	—	—	650	—	380

followed by a slow change at higher exposures (Fig. 4A). The maximum work function decrease was about 1.8 eV. Heating the adsorbed layer of C_2H_5I resulted in a steep increase in the work function up to 300 K, when the work function of the sample exceeded by about 0.4 eV that of the undosed surface (Fig. 4B). The value of the initial sample was attained above 800 K.

3.2.2. XPS measurements. Exposing the Mo_2C/Mo(111) sample to C_2H_5I at 90 K the binding energy of I($3d_{5/2}$) appeared at 620.5 eV and did not change with the variation of C_2H_5I exposure. The area of the I($3d_{5/2}$) (XPS) peak at 620.5 eV increased linearly with the exposure. In the C(1*s*) region, the adsorption of C_2H_5I produced a new broad peak centered at 284.5 eV.

Selected XPS spectra of adsorbed layers annealed at different temperatures are displayed in Fig. 5A. Annealing of a multilayer below 150 K caused only a slight change in the I($3d_{5/2}$) and C(1*s*) XPS spectra. A new peak, 618.9 eV, for I($3d_{5/2}$) can be traced even at 150 K, but its clear appearance occurred at 190 K. The peak at 620.5 eV became undetectable above 275 K.

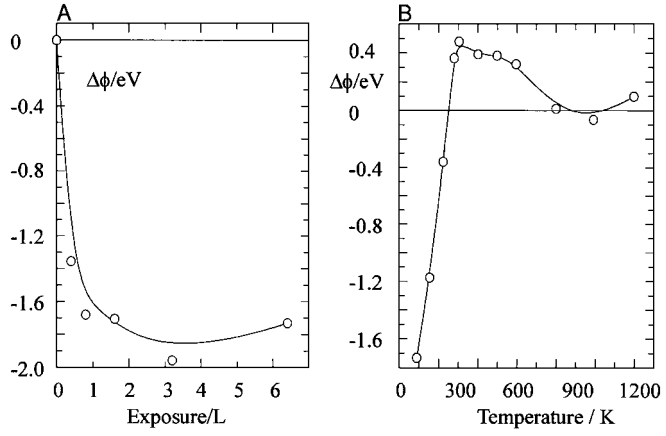

FIG. 4. Changes in the work function ($\Delta\phi$) of Mo_2C/Mo(111) (A) as a function of C_2H_5I exposure at 100 K (B) and annealing temperature.

3.2.3. TPD measurements. Figure 6A shows TPD spectra of C_2H_5I at different exposures. Desorption of molecularly adsorbed C_2H_5I was observed above 0.8 L; a single desorption peak developed with $T_p = 145$ K. The position of the peak remained practically unaltered with increasing C_2H_5I exposure and did not reach saturation. No other C_2H_5I desorption state was established.

Besides the desorption of C_2H_5I, the formation of C_2H_6 and C_2H_4 was also observed (Figs. 6B and 6C). The amount of C_2H_6 increased with the increase of C_2H_5I coverage up to ~3.0 L of C_2H_5I exposure and its peak temperature, 250 K, remained unaltered. Ethylene desorbed in two peaks. The low temperature peak (α) appeared always at 230–265 K, whereas the high temperature peak (β) shifted from 545 to 455 K with the increase of C_2H_5I exposure. Saturation of both compounds was attained at ~3.0 L. Taking into account the sensitivity of the mass spectrometer to the products of C_2H_5 decomposition, we obtained that the total amount of ethylene formed was ~2.5 times higher than that of ethane. Attempts to identify the formation of other hydrocarbon products (butane and methane) did not bring positive result. The desorption of H_2, however, also occurred with $T_p = 405$ K and $T_p = 580$ K. When the adsorption of C_2H_5I was performed at 300 K, we experienced a marked difference in the product distribution. The absolute and relative amounts of ethylene increased and ethane was practically absent in the products.

The peak temperatures and the activation energies of the desorption of various products are given in Table 1, while the effect of adsorption temperature on the product distribution is summarized in Table 2.

3.2.4. HREELS measurements. HREEL spectra were recorded in the specular direction for C_2H_5I as a function

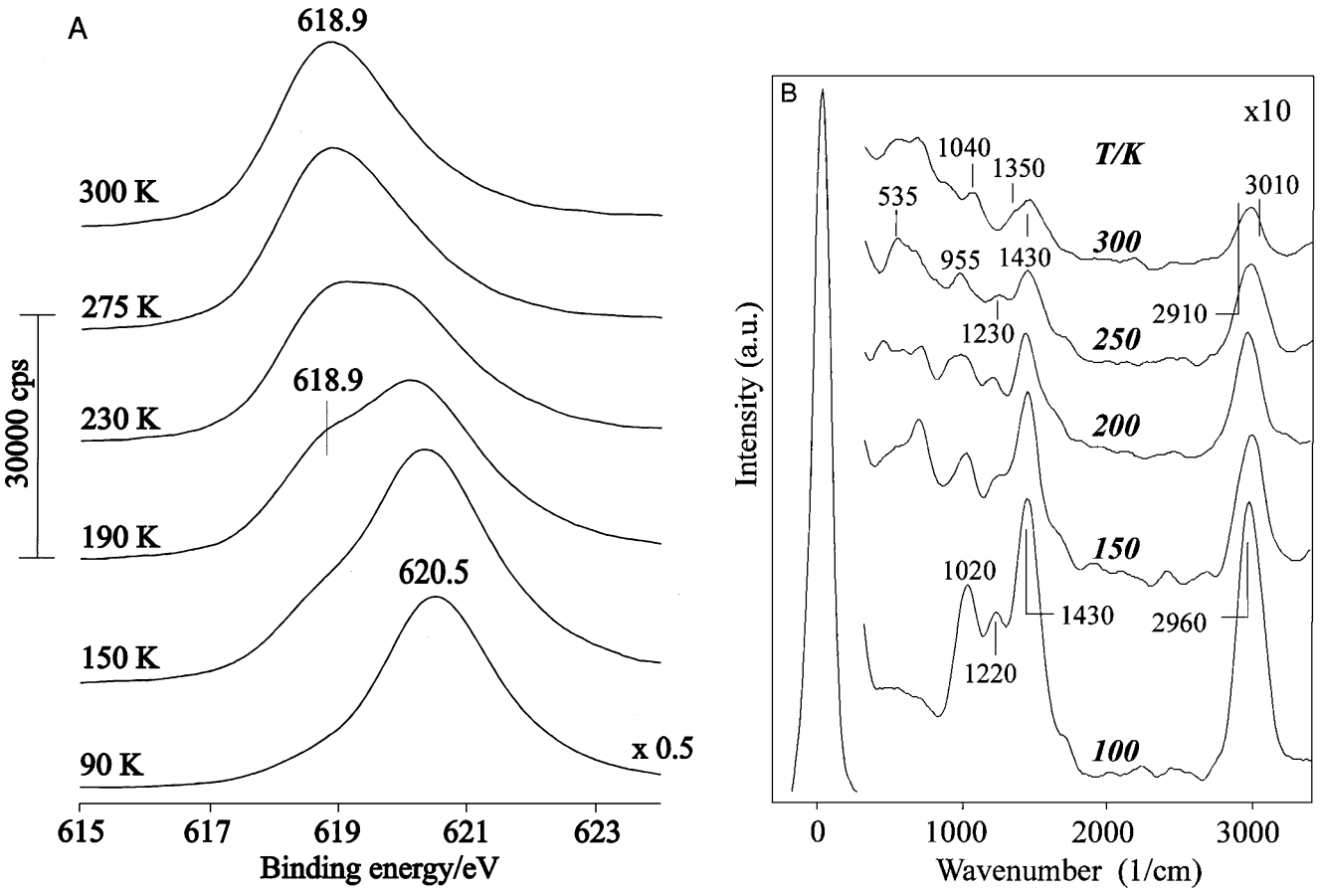

FIG. 5. Effects of annealing on (A) the XPS spectra of I($3d_{5/2}$) and (B) on HREEL spectra of adsorbed C_2H_5I.

of exposure at 100 K. Vibration losses were resolved at 2960, 1430, 1225, and 1020 cm^{-1} (Fig. 5B). The positions of the losses did not exhibit any dependence on the coverage. Loss features for C_2H_5I adsorbed on the Mo_2C/Mo(111) surface are listed in Table 4, which contains the vibrational characteristics of gaseous C_2H_5I and C_2H_5I adsorbed on Rh(111), too.

TABLE 4

Vibrational Frequencies of Gaseous C_2H_5I and Adsorbed C_2H_5I and C_2H_5

	$C_2H_5I_{(g)}$ (45)	C_2H_5I/Rh(111) (45)	C_2H_5/Rh(111) (8, 45)	C_2H_5I/Mo_2C/Mo(111) at 100 K (present work)
ν(C-H)	2968	2950	2910	2960
$\delta(CH_3)$	1452	1453	1420	1430
$\delta(CH_2)$				
$\omega(CH_2)$	1199	1220	1150	1220
ν(C-C)	949	1000	940	1025
$\rho(CH_3)$			850	
$\rho(CH_2)$	736	760		
ν(C-I)	496	516		
ν(M-C)			395	
ν(M-I)		260		

The HREELS anneling set of adsorbed C_2H_5I is shown in Fig. 5B. At 150 K, a significant attenuation of the losses was registered and at the same time the development of a feature at 700 cm^{-1} was observed. At 200 K other new loss features appeared at 435 and 955 cm^{-1}. At 250 K the 435 cm^{-1} feature moved to 533 cm^{-1}, and the 1020 cm^{-1} peak was absent. Note that the 1220 cm^{-1} loss was still present on the spectrum up to that temperature, it disappeared only at 300 K. The loss at 2960 cm^{-1} became clearly broader at 250–300 K, and a low and a high frequency shoulder may be resolved.

When the surface was exposed to C_2H_5I at 300 K and heated up to higher temperatures, we observed the same loss features as in the case of the adsorption of CH_2I_2 under the same conditions.

4. DISCUSSION

4.1. Properties of Transition Metal Carbides

Interstitial carbides of early transition metals (groups IVB–VIB) have unique physical and chemical properties

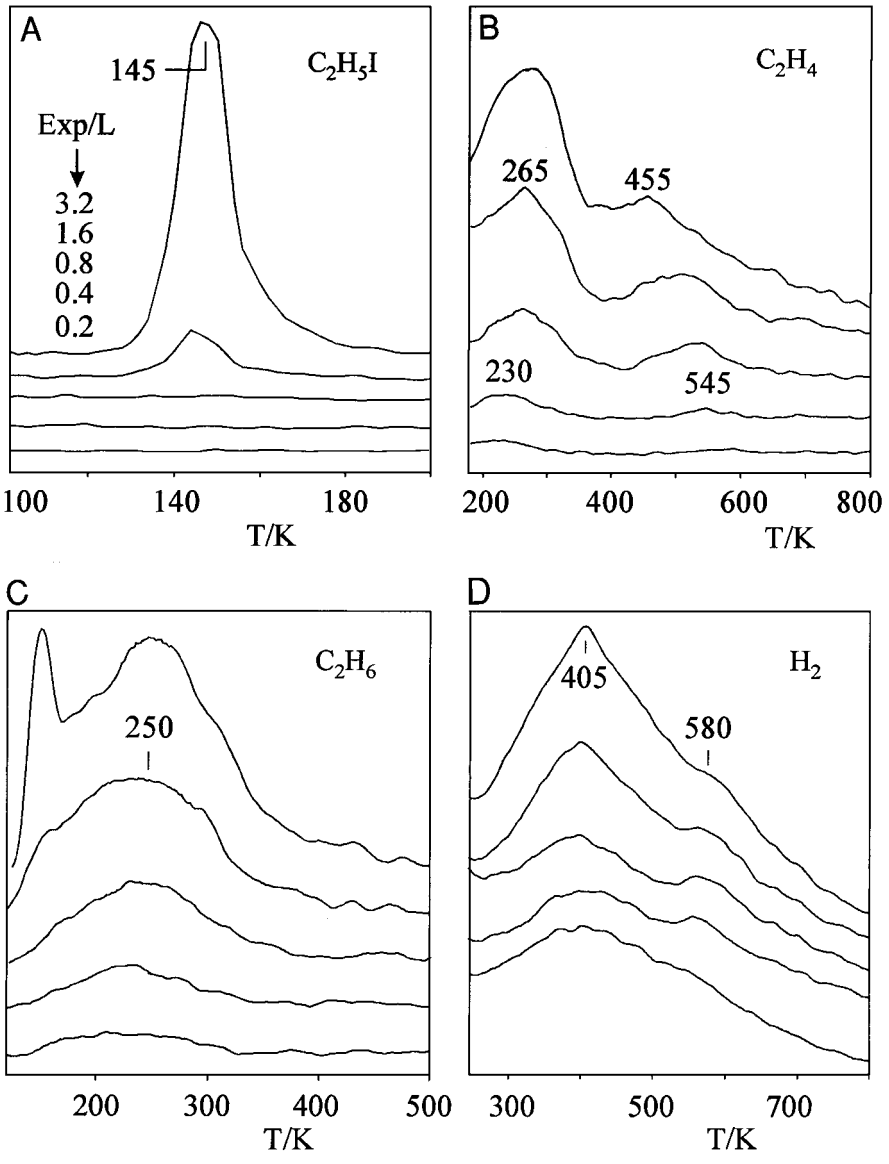

FIG. 6. TPD spectra following C_2H_5I adsorption on Mo_2C/Mo(111) at 100 K as a function of C_2H_5I exposure. (A) C_2H_5I; (B) C_2H_4; (C) C_2H_6; (D) H_2.

(35–37). This is particularly valid to Mo_2C, the catalytic activity of which in certain cases approaches, and even surpasses, those of noble metals (37, 38). Recently, the surface properties and the adsorption of several gases have been extensively investigated by using the tools of modern surface science (39–41). The results obtained are well documented in a recent review (40).

4.2. *Chemistry of CH_2I_2 on Mo_2C*

4.2.1. Adsorption and dissociation of CH_2I_2. The adsorption of CH_2I_2 on Mo_2C/Mo(111) is characterized by a decrease in work function ($\Delta\phi = 0.9$ eV), indicating that adsorbed CH_2I_2 has a positive outward dipole moment. This feature is consistent with the bonding of molecular alkyl and alkene halides through the halogen atom, since these molecules all have permanent dipoles with the CH_x group positive. We may assume that the loose structure of carbon overlayer over Mo allows the formation of a direct bonding between Mo and I ends of CH_2I_2 molecules. The formation of Mo–I bond is supported by the high desorption temperture of I from the Mo_2C/Mo(111) surface ($T_p = 1100$ K). Nearly the same peak temperatures were measured for I desorption following the adsorption of iodo compounds on transitional metal surfaces (8), which reflects the strong bond between the metals and adsorbed I. Interestingly, the work function of the system is increased by about 0.3 eV, at and above 1.6 L exposure, when the desorption of CH_2I_2

was detected by TPD. This feature is very likely due to the less ordered arrangement of permanent dipoles in the second (multi) layer.

By means of TPD measurements, we found only one adsorption state, which could not be saturated and desorbed with $T_p = 195$ K. This is the characteristic feature of the formation of a multilayer. The activation energy calculated for this desorption process is 50.0 kJ/mol. The peak temperature for the desorption of multilayer agrees with those registered on Pd(100) and Rh(111) surfaces (42, 43). The fact that at low exposures there was no desorption of CH_2I_2 suggests that a more stable state also exists on the surface which instead of desorption undergoes decomposition at higher temperatures.

HREEL spectra of adsorbed CH_2I_2 for different coverages at 100 K correspond well to those measured for gaseous CH_2I_2 or for molecularly adsorbed CH_2I_2 on Rh(111) (Table 3). It appears that the modes involving the CH_2 group are not significantly altered from their gas-phase values. Accordingly the losses observed are assigned to $\nu_{as}(CH_2)$ (3030 cm^{-1}), $\delta(CH_2)$ (1360 cm^{-1}), $\gamma(CH_2)$ (1080 cm^{-1}), $\rho(CH_2)$ (675 cm^{-1}), and ν_{as}(C-I) (580 cm^{-1}).

In the XP spectra, adsorbed CH_2I_2 is characterized by a I($3d_{5/2}$) binding energy of 620.0 eV and by a C(1*s*) binding energy of 285.1 eV which were independent of the coverage. These values are nearly the same as observed for molecular adsorption of CH_2I_2 on Pd(100) and Rh(111) surfaces (42, 43). Note that the binding energy of I($3d_{5/2}$) is very sensitive to the nature of I, and its value is the best indication for the occurrence of the dissociation of the C–I bond. The binding energy of I($3d_{5/2}$) in atomically adsorbed state on metal surfaces is between 618.5 and 619.7 eV. In the present case, this low binding energy of I($3d_{5/2}$) was not seen even at submonolayer coverage. All these data of HREELS and XPS measurements performed at 100 K suggest that CH_2I_2 adsorbs molecularly on Mo_2C/Mo(111) at this temperature.

A shift in the binding energy for I($3d_{5/2}$) was, however, detected first at 170 K, indicating the dissociation of CH_2I_2 on Mo_2C/Mo(111). The molecularly adsorbed CH_2I_2 was present in rather wide temperature range as the high energy XPS signal at 620.1 eV, characteristic for adsorbed CH_2I_2, disappeared only above ~250 K (Fig. 2A). Note that the work function of the system is still lower by about 0.55 eV for the annealed layer at 250–450 K (Fig. 1B), when the desorption of the weakly adsorbed CH_2I_2 and possibly the dissociation of CH_2I_2 are complete. For this feature the hydrocarbons formed in the reactions of CH_2 should be responsible as the atomically adsorbed I remaining on the surface above 600 K slightly increases the work function of Mo_2C/Mo(111) sample (Fig. 1B).

In the HREEL spectra the first spectral indication for the change in the adsorbed layer appeared at 222–280 K, where a peak at 1190 cm^{-1} and shoulders at 800 and 2940 cm^{1} could be resolved in the spectrum: all these features can be attributed to the vibrations of CH_2 species produced by the dissociation of CH_2I_2 (Table 3).

4.2.2. Reactions of CH_2 species on Mo_2C. TPD measurements clearly demonstrated that CH_2 formed in the dissociation of CH_2I_2 undergoes reactions on the Mo_2C/Mo(111) surface. The most important feature is the production of ethylene in relatively larger quantity compared to the case of Rh(111) and Pt(111) (8). This feature also differs from that observed for clean Mo(110) and (100) surfaces, where only the hydrogenation of CH_2 into methane was observed without a detectable coupling reaction (45). On MoO_x film, however, the CH_2 species produced by photodissociation gave C_2H_4 and CH_2O, too (46). This suggests that the coupling of CH_2 species,

$$2\,CH_{2(a)} = C_2H_{4(a)},$$

is a more favorable step on Mo_2C than on the above metals.

The analysis of HREEL spectra reveals that the coupling of CH_2 species proceeds above 280 K, or more precisely the presence of adsorbed ethylene can be clearly detected above this temperature. The vibrational features, 1390, 1030, 870–900, and 630 cm^{-1} observed at 310–420 K (Fig. 2B) correspond well to the di-σ-bonded ethylene (Table 3). Recently, Frühberger and Chen (44) reported that ethylene molecules bond to Mo_2C/Mo(110) surface in the di-σ-bonded configuration even at lower temperatures, and it transforms into ethylidyne species at higher temperatures. The formation of ethylidyne was indicated by the vibrational losses at 2915, 1430, 1075, 920, and 525 cm^{-1}. Although the surface concentration of di-σ-bonded ethylene is obviously much lower than that seen in the referred study (44), when Mo_2C surface has been exposed to pure ethylene, weak signals observed in the HREEL spectra of annealed layer above 420 K suggest that we can count with the formation of ethylidyne in the present case, too, which is not a surprising result.

Accordingly, the high temperature of ethylene desorption may be explained by the back reaction of ethylidyne and hydrogen:

$$C \cdot CH_{3(a)} + H_{(a)} = C_2H_{4(g)}.$$

This process was also observed on Pd(100) (42). In addition to ethylene, the desorption of methane was also registered with $T_p = 300$ K. This high desorption temperature suggests that its formation is a reaction limited process. The methane formation may be described by the reaction

$$3\,CH_{2(a)} = CH_{4(g)} + 2\,CH_{(a)}.$$

As in other cases, we may assume that the hydrogen in the background also contributes to the hydrogenation of CH_x fragments.

The formation of hydrogen with $T_p = 380$–400 K suggests that a fraction of CH_2 species decomposes to carbon:

$$CH_{2(a)} = C_{(a)} + 2\,H_{(a)}.$$

The release of a small amount of hydrogen above 500 K is probably the result of the decomposition of unreacted ethylidyne or CH species:

$$C \cdot CH_{3(a)} = CH_{(a)} + C + H_{2(g)}$$
$$2\,CH = 2\,C + H_{2(g)}.$$

4.3. *Chemistry of C_2H_5I on Mo_2C*

4.3.1. Adsorption and dissociation of C_2H_5I. The adsorption of C_2H_5I on Mo_2C also led to a decrease in work function (~1.6 eV), indicating that the nature of the adsorption of C_2H_5I is similar to that of CH_2I_2.

By means of TPD measurements, we observed only the formation of a multilayer desorbing at very low temperature, $T_p = 145$ K. The peak temperature was independent of the coverage, which indicates first-order desorption kinetics. The activation energy calculated via the Redhead formula is 36.0 kJ/mol.

The features of HREEL spectra registered for adsorbed C_2H_5I on Mo_2C/Mo(111) at 100 K agree well with those attributed to C_2H_5I. The assignments of the vibration losses are presented in Table 4. This suggests that the adsorption of C_2H_5I on Mo_2C/Mo(111) at 100 K is molecular. Following the adsorption of C_2H_5I by XPS at 100 K we obtained a peak for I($3d_{5/2}$) at 620.5 eV, the position of which was independent of the coverage. Taking into account the previous consideration (see Section 4.2.1), this value also speaks for the molecular adsorption at C_2H_5I at 100 K. In the region of binding energy for C(1*s*), the adsorption of C_2H_5I yielded a new peak at 284.5 eV.

The dissociation of molecularly bonded C_2H_5I occurred to a well detectable extent at 180 K. This is clearly exhibited by the appearance of a new binding energy for I($3d_{5/2}$) at 618.9 eV and the attenuation of the peak at 620.5 eV. This latter peak is not resolvable above 250 K, when the low BE peak dominated the spectrum. This spectral change was not accompanied by any appreciable alteration of the C(1*s*) peak at 284.5 eV.

In harmony with this, spectral changes in the HREELS of adsorbed C_2H_5I were also established at about 200 K, which can be associated with the cleavage of the C–I bond. As in the previous case, however, we can count with the coexistence of several adsorbed species, which prevented the unambiguous identification of C_2H_5: only the appearance of a vibrational loss at 955 cm^{-1} can be clearly attributed to this species (Table 4).

4.3.2. Reactions of C_2H_5 species. TPD measurements clearly demonstrated that C_2H_5 formed in the dissociation of C_2H_5I undergoes reactions on the Mo_2C/Mo(111) surface. The product distribution is different from that observed for CH_2 reactions, as CH_4 is missing and C_2H_6 is produced. The latter compound starts desorbing above 180 K with $T_p = 250$ K. We observed the same peak temperature for desorption of C_2H_6 following its adsorption on Mo_2C/Mo(111) surface at 100 K, which may suggest that the desorption of C_2H_6 is a desorption limited process. Another product is ethylene, the desorption of which begins at 180–200 K with a $T_p = 230$–270 K. A high temperature ethylene peak was also registered at $T_p = 545$–455 K (Fig. 6). The formation of these compounds at rather low temperature suggests that the dehydrogenation and hydrogenation of C_2H_5,

$$C_2H_{5(a)} = C_2H_{4(a)} + H_{(a)}$$
$$C_2H_{5(a)} + H_{(a)} = C_2H_{6(a)},$$

proceed immediately after its formation, which prevented or made difficult its spectroscopic identification. As in the case of Rh(111) (47), it is very likely that the background hydrogen also participates in the latter process.

Interestingly, in the reaction of CH_2 we observed no low temperature desorption of C_2H_4. The possible reason for the difference is that in the case of CH_2 the coupling of CH_2 should occur first, which involves the migration of adsorbed CH_2 species. In the case of C_2H_5 the C–C bond is given, and the formation of ethylene requires only the dehydrogenation of C_2H_5, which occurs easily on Mo_2C. The formation and desorption of C_2 compounds at lower temperatures causes the increase in the work function of the sample at significantly lower temperatures compared to the case of CH_2I_2 (Fig. 4B). The low value of T_p for C_2H_5I desorption, however, also contributes to this phenomenon.

In contrast with the Ag(111) surface (48), no recombination of C_2H_5 into C_4H_{10} occurred, which is connected with the good dehydrogenating and hydrogenating properties of Mo_2C.

The desorption of ethylene and hydrogen at high temperatures as well as the spectroscopic features observed in HREEL spectra after annealing the adsorbed layer above 300 K suggest that a fraction of ethylene produced undergoes similar processes as described in Section 4.2.

4.4. *Comparison of the Behavior of CH_x Fragments on Mo_2C and Pt Metal Single Crystals*

As was mentioned in the Introduction, all the Pt metals were found quite effective in breaking the C–I bond in the adsorbed CH_2I_2 and C_2H_5I (3–9). Mo_2C/Mo(111) sample is less reactive: the rupture of the C–I bonds in these compounds was observed at 140–170 K, and the dissociation of the entire adsorbed layer requires higher temperature. A similar feature was observed for CH_3I (26). On Pt metals the hydrocarbon fragments (CH_2 and CH_3) formed in the dissociation of iodo compounds underwent fast

decomposition, producing only minor quantities of C_2 compounds. On Mo_2C, however, the tendency of the coupling of CH_2 into C_2H_4 is much greater than on these metals. Surprisingly, the formation of C_2H_4 also occurred in the reaction of adsorbed CH_3 on Mo_2C, which was not detected at all for Pt metals (26).

The reaction pathways of adsorbed C_2H_5 did not differ much on Pt metals and Mo_2C. While the C–C bond remained intact, both the dehydrogenation and the hydrogenation of C_2H_5 proceeded. The relative amount of ethylene was, however, somewhat higher on Mo_2C.

Bearing these features in mind, we may understand the completely different reaction route of methane on supported Mo_2C compared to supported Pt metals. In the latter case the CH_x fragments produced in the first activation step in the CH_4 dissociation decompose very rapidly to surface carbon. This behavior is practically independent of the support (22–25). Mo_2C can also activate the methane molecule, but the lifetime of the CH_x fragments is longer than on Pt metals, so they can recombine and undergo further reactions now on the surface of suitable supports (ZSM-5 and SiO_2) to give aromatic compounds.

5. CONCLUSIONS

(i) CH_2I_2 and C_2H_5I adsorb molecularly on Mo_2C/Mo(111) at 100 K, leading to a decrease of the work function by 0.9 and 1.8 eV, respectively.

(ii) The dissociation of the compounds started at 150–190 K, resulting in the formation of adsorbed CH_2 and C_2H_5.

(iii) A fraction of CH_2 is hydrogenated into methane and another fraction recombined into ethylene, which desorbed with $T_p = 440$ and 530 K.

(iv) C_2H_5 underwent hydrogenation and dehydrogenation to give ethane and ethylene.

(v) The elevation of the adsorption temperature from 100 K to 300 K increased the amount of desorbed ethylene in both cases. The extent of the formation of adsorbed ethylene from CH_2(a) is significantly larger than that observed for Pt metals.

(vi) Ethylene formed in the reactions of both C_xH_y fragments appeared as di-σ-bonded ethylene, which is transformed into ethylidyne, $C \cdot CH_3$, at higher temperature.

ACKNOWLEDGMENT

This work was supported by Grant OTKA Nr 022869.

REFERENCES

1. Bibby, D. M., Chang, C. D., Howe, R. F., and Yurchak, S. (Eds.), *in* "Studies in Surface Science and Catalysis" (B. Delmon and J. T. Yates, Jr., Eds.), Vol. 36. Elsevier, Amsterdam, 1988.
2. Lunsford, J. H., "Proceedings of 10th International Congress on Catalysis, Budapest, 1992" (L. Guczi, F. Solymosi, and P. Tétényi, Eds.), Akadémiai Kiadó, Budapest, 1993.
3. Zaera, F., *Acc. Chem. Res.* **25**, 260 (1992).
4. Zaera, F., *J. Mol. Catal.* **86**, 221 (1994).
5. Solymosi, F., *Catal. Today* **28**, 193 (1996).
6. Bent, B. E., *Chem. Rev.* **96**, 1361 (1996).
7. Solymosi, F., Berkó, A., and Révész, K., *Surf. Sci.* **240**, 59 (1990).
8. Solymosi, F., *in* "Catalytic Activation and Functionalism of Light Alkane" (E. G. Derouane *et al*., Eds.). Kluwer Academic, Dordrecht, 1998.
9. Solymosi, F., *J. Mol. Catal. A* **131**, 121 (1998).
10. Zhou, X.-L., Zhou, X.-Y., and White, J. M., *Surf. Sci. Rep.* **13**, 73 (1001).
11. Solymosi, F., Kiss, J., and Révész, K., *J. Phys. Chem.* **94**, 2224 (1990).
12. Solymosi, F., Kiss, J., and Révész, K., *J. Chem. Phys.* **94**, 8510 (1991).
13. Costello, S. A., Roop, B., Liu, Z. M., and White, J. M., *J. Phys. Chem.* **92**, 1019 (1988).
14. Berkó, A., and Solymosi, F., *J. Phys. Chem.* **93**, 12 (1989).
15. Kiss, J., Berkó, A., Révész, K., and Solymosi, F., *Surf. Sci.* **240**, 59 (1990).
16. Kovács, I., Iost, N., and Solymosi, F., *J. Chem. Phys.* **101**, 4236 (1994).
17. van Santen, R. A., de Koster, A., and Koerts, T., *Catal. Lett.* **7**, 1 (1990).
18. Koerts, T., Deelen, M. J. A. G., and van Santen, R. A., *J. Catal.* **138**, 101 (1992).
19. Belgued, M., Pareja, P., Ameriglio, A., and Ameriglio, H., *Nature* **352**, 789 (1991).
20. Belgued, M., Pareja, P., Ameriglio, A., Ameriglio, H., and Saint-Just, J., *Catal. Today* **13**, 437 (1992).
21. Solymosi, F., Kutsán, Gy., and Erdőhelyi, A., *Catal. Lett.* **11**, 149 (1991).
22. Solymosi, F., Erdőhelyi, A., and Cserényi, J., *Catal. Lett.* **16**, 399 (1992).
23. Erdöhelyi, A., Cserényi, J., and Solymosi, F., *J. Catal.* **141**, 287 (1993).
24. Solymosi, F., Erdőhelyi, A., Cserényi, J., and Felvégi, A., *J. Catal.* **147**, 272 (1994).
25. Solymosi, F., and Cserényi, J., *Catal. Today.* **21**, 561 (1994).
26. Solymosi, F., Bugyi, L., and Oszkó, A., *Catal. Lett.* **57**, 103 (1999).
27. Wang, D., Lunsford, J. H., and Rosynek, M. P., *Topics Catal.* **3**(4), 299 (1996).
28. Solymosi, F., and Szöke, A., *Catal. Lett.* **39**, 157 (1996).
29. Solymosi, F., Cserényi, J., Szöke, A., Bánsági, T., and Oszkó, A., *J. Catal.* **165**, 150 (1997).
30. Wang, D., Lunsford, J. H., and Rosynek, M. P., *J. Catal.* **169**, 347 (1997).
31. Wang, L., Tao, L., Xie, M., and Xu, G., *Catal. Lett.* **21**, 35 (1993).
32. Xu, Y., Liu, S., Wang, L., Xie, M., and Guo, X., *Catal. Lett.* **30**, 135 (1995).
33. Solymosi, F., Erdőhelyi, A., and Szöke, A., *Catal. Lett.* **32**, 43 (1995).
34. Schöberl, Th., *Surf. Sci.* **327**, 285 (1995).
35. Leclercq, L., *in* "Surface Properties and Catalysis by Nonmetals" (J. P. Bonelle, B. Delmon, and E. G. Derouane, Eds.). Reidel, Dordrecht, 1993.
36. Djega-Mariadassou, G., *in* "Catalytic Activation and Functionalism of Light Alkane" (E. G. Derouane, J. Haber, F. Lemos, F. R. Riberio, and M. Guisnet, Eds.). Kluwer Academic, Amsterdam 1998.
37. Oyama, S. T., *Catal. Today* **15**, 179 (1992).
38. Ledoux, J. M., Phom Huu, C., Guille, J., and Dunlop, H., *J. Catal.* **134**, 383 (1992).
39. Johansson, L. I., *Surf. Sci. Rep.* **21**, 177 (1995) and references therein.
40. Chen, J. G., *Chem. Rev.* **96**, 1477 (1996) and references therein.
41. Chen, J. G., Frühberger, B., Eng, J., Jr., and Bent, B. E., *J. Mol. Catal. A* **131**, 285 (1998).
42. Solymosi, F., and Kovács, I., *Surf. Sci.* **296**, 171 (1993).
43. Solymosi, F., and Klivényi, G., *Surf. Sci.* **342**, 8950 (1995).
44. Frühberger, B., and Chen, I. G., *J. Am. Chem. Soc.* **118**, 11599 (1996).
45. Wu, G., Bartlett, B. F., and Tysoe, W. T., *Surf. Sci.* **373**, 129 (1997); Weldon, M. K., and Friend, C. M., *Surf. Sci. Lett.* **321**, L202 (1994).
46. He, H., Nakamura, J., Takehiro, N., and Tanaka, K., *J. Vac. Sci. Technol. A* **13**, 2689 (1995).
47. Bugyi, L., Oszkó, A., and Solymosi, F., *Langmuir* **12**, 4145 (1996).
48. Zhou, X.-L., and White, J. M., *Catal. Lett.* **2**, 375 (1989).